frontiers | Frontiers in Environmental Science

TYPE Review
PUBLISHED 15 January 2026
DOI 10.3389/fenvs.2025.1746525

OPEN ACCESS

EDITED BY
Pietro Paolo Falciglia,
University of Catania, Italy

REVIEWED BY
Oscar Manuel Rodriguez Narvaez,
Centro de Innovación Aplicada en Tecnologías Competitivas (CIATEC), Mexico
Kiyan Sorgog,
University of Mississippi Medical Center, United States

*CORRESPONDENCE
Andrea Luca Tasca,
andrea.luca.tasca@associated.ltu.se

RECEIVED 14 November 2025
REVISED 23 December 2025
ACCEPTED 24 December 2025
PUBLISHED 15 January 2026

CITATION
Tasca AL, Uwayezu JN, Panizza M, Kumpiene J and Carabante I (2026) PFAS removal by ultrasound irradiation: pathways, chemistry and operation.
Front. Environ. Sci. 13:1746525.
doi: 10.3389/fenvs.2025.1746525

PFAS removal by ultrasound irradiation: pathways, chemistry and operation

Andrea Luca Tasca[1]*, Jean Noel Uwayezu[1], Marco Panizza[2], Jurate Kumpiene[1] and Ivan Carabante[1]

[1]Department of Civil, Environmental and Natural Resources Engineering, Luleå University of Technology, Luleå, Sweden, [2]Department of Civil, Chemical and Environmental Engineering, University of Genoa, Genoa, Italy

Per- and polyfluoroalkyl substances (PFAS) are synthetic chemicals found worldwide in several industrial and consumer products. The extensive use of these fluorinated organic compounds, together with their high stability, has led to a broad contamination of water and soil resources. Among the technologies under development for their remediation, sonochemistry stands out. Propagation of ultrasounds in aqueous media results in sonophysical and sonochemical effects, able to collaboratively mineralize most of PFAS. Oxidative additives, as well as surfactants, may enhance the performance of the technique, which is also affected by organic matter, residual solvents, pH and temperature of the solution. PFAS concentration is a crucial factor in terms of treatment efficiency since it defines the rate order, while differences in functional group, chain length, and extent of fluorination affect hydrophobicity, surface activity and thermal activation energy of PFAS. Reaction pathways, solution chemistry, reactor configuration, and operational parameters including flowrate, atmosphere condition, US frequency and power density are discussed within this critical review, with the aim of boosting the implementation of this technology for PFAS remediation.

KEYWORDS

per- and polyfluoroalkyl substances, review, sonolysis, ultrasounds, water treatment

1 Introduction

Per- and polyfluoroalkyl substances (PFAS) are synthetic chemicals manufactured since the 1940s (Das and Ronen, 2022), extensively used in several industrial and consumer products. PFAS molecules include the perfluoroalkyl group (C_nF_{2n+1}), frequently $C4-C8$ in length and arranged linearly. Perfluoro chains with different length, branched, and with some not-fluorinated carbons have also been developed. The strength (≈440–530 kJ mol^{-1}) and the short length (≈1.3–1.4 Å) of $C-F$ bonds, as well as electrostatic and steric shielding of $C-C$ bonds by fluorine atoms (Lenka et al., 2021), confer to these compounds an extreme stability. PFAS fluorinated tail is hydrophobic, while the non-fluorinated headgroup is typically hydrophilic, conferring to most of these compounds surfactant-like properties. Variations in fluorination, length, branching, and headgroup distinguish several different structures, giving specificity for multiple applications, including non-stick cookware, stain- and water-resistant products, food packaging, and firefighting foam (Lenka et al., 2021; Verma et al., 2023).

The extensive use of PFAS across several industries, combined with their exceptional stability, has led to worldwide contamination of water and soil resources (Sivagami et al.,

2023). Temporal trends investigated on water, sediments, birds, fish, marine mammals and humans show how the exposure to these compounds has risen over the last 3 decades (Ahmed et al., 2020). These fluorinated organic compounds have been associated with adverse health implications, such as liver damage, endocrine disruption, thyroid illness, decreased fertility, and cancer (Verma et al., 2023).

Low removal efficiencies have been found in most wastewater treatment plants, and several investigations reported an increase in the levels of PFAS after treatment (Lenka et al., 2021). Indeed, some PFAS are partially degraded to form other polyfluorinated compounds, as well as *in-situ* generation from precursors occurs. Moreover, the gradual substitution of long-chain compounds due to their persistence, bioaccumulation, and toxicity (Karatas et al., 2023; Li et al., 2023; Saleh et al., 2024) with short chain analogues resulted in new challenges to be faced (Olvera-Vargas et al., 2022). Indeed, nowadays, short-chain PFAS are widely detected in the environment (Mirabediny et al., 2023), while the knowledge of remediation techniques available for these pollutants is still limited (Asadi Zeidabadi et al., 2024).

Legislation is becoming more and more stringent worldwide (Yu et al., 2025). Research is focusing on the modification of conventional remediation technologies, as well as on the development and advancement of innovative techniques. Adsorption and filtration are applied to separate PFAS from several effluents (Vakili et al., 2024). In recent years, foam fractionation is also emerging as a promising technology to concentrate PFAS from aqueous streams (We et al., 2024). However, an additional step is required to treat the spent adsorbent or concentrated retentate (Vakili et al., 2024), as well as PFAS-enriched fractionated foam.

Hence, destructive technologies are needed to achieve complete PFAS mineralization. Among them, electrochemical degradation (Tasca et al., 2025) and ultrasound irradiation (Marín-Marín et al., 2023) stand out. Electrochemical degradation involves direct anodic oxidation, as well as the generation of highly reactive species through indirect anodic oxidation (Tasca et al., 2025). Propagation of ultrasounds (US), i.e., sound waves with frequencies higher than 20 kHz, vibrates liquids at high speeds, resulting in micro to nano scale ruptures or voids inside the bulk matrix. The phenomenon is known as cavitation. Micro-to nano-sized bubbles grow and collapse violently when they reach the maximum resonant size (Lauterborn and Mettin, 2023; Pétrier and Wei, 2023). The implosion of these acoustic cavities produces locally very high temperature and pressure. Related sonophysical and sonochemical effects (Khoshyan et al., 2024) offer the potential to collaboratively degrade even the most recalcitrant organic compounds. Among them, the complete mineralization of PFAS into aqueous contaminated media into harmless inorganics has been demonstrated by several studies (Sidnell et al., 2022).

Within this critical review, the efficiency of the treatment of PFAS-contaminated aqueous media performed by US irradiation is related to PFAS initial concentration, chain length, headgroup, and characteristics of the bulk matrix. Degradation mechanism and pathways are presented. The effect of power density, ultrasonic frequency, flowrate, pH, temperature and additives are described. Finally, synergic combination with remediation techniques and future research directions are discussed.

2 Mechanism

Cavitation bubbles resulting from US irradiation grow rapidly until absorption of US energy from the acoustic wave is possible, then collapse (Suslick, 1989), producing locally extreme temperatures (up to 5000–10000 K) and pressures (up to 60000 atm). This phenomenon is accompanied by sonophysical effects, such as microjets, microstreaming, and shock waves, as well as sonochemical effects, including pyrolysis, and radical reaction (Khoshyan et al., 2024). Before bubble collapse, PFAS adsorption at the air-water interface may occur, with the hydrophilic headgroup preferring the liquid medium and the hydrophobic perfluoro tail entering the gas phase (Moriwaki et al., 2005) (Figure 1a). This hypothesis is supported by bubble saturation kinetics reported at increasing concentrations (Fernandez et al., 2016; Rodriguez-Freire et al., 2015; Shende et al., 2019; Vecitis et al., 2010). Headgroup pyrolytic cleavage follows upon bubble collapse, mainly due to high inner/interfacial bubble temperature, solvated electron release, or both (Figure 1b) (Sidnell et al., 2022). Headgroup cleavage has been confirmed by the production of SO_4^{2-} and short chain PFAS (Fernandez et al., 2016; Lin et al., 2016; Moriwaki et al., 2005; Rodriguez-Freire et al., 2015; Shende et al., 2019; Vecitis et al., 2010). Accordingly, PFAS degradation rate is limited by the available bubble surface area, rate of compounds adsorption at the bubble surface, and rate of headgroup cleavage. Concerning the cleaved perfluoroalkyl chain, it may degrade by plasma/pyrolysis reactions inside the bubble in a single collapse event, with eventual generation of by-products from recombination of fragments in the liquid matrix (Vecitis et al., 2008a) (Figure 1c1). Otherwise, oxidation of the truncated tails in the liquid bulk may also occur. Shortened Perfluoroalkyl Carboxylic Acids (PFCAs) are formed (even from the degradation of Perfluoroalkane Sulfonic Acids, i.e., PFSAs) and adsorb to new bubbles. The process may repeat, with the cleavage of one CF_2 group per cycle (Moriwaki et al., 2005) (Figures 1a-b-c2 loop). Formation of intermediates (Figure 1d) and their hydrolysis to end products in liquid phase (Figure 1e) follow.

This mechanism is generally agreed for both PFCAs and PFSAs at mid-high frequencies (100–1,000 kHz). Very recently, thermolysis has been confirmed to be the primary degradation pathway under US irradiation also of fluorotelomer sulfonates (FTSAs) (Fagan et al., 2023). Pathways at low frequency are more varied and still not clearly assessed, due to the various oxidants utilized to enhance the degradation (Sidnell et al., 2022).

3 Measurements

PFAS sonolysis results mainly in F^-, SO_4^{2-}, CO, CO_2 (James Wood et al., 2020; Shende et al., 2019; Singh Kalra et al., 2021; Vecitis et al., 2010), and short chain or partially fluorinated products (Gole et al., 2018b; James Wood et al., 2020; Panda et al., 2019; Rodriguez-Freire et al., 2016). However, the measurement of inorganic species does not necessarily quantify the extent of mineralization. Indeed, sulfur balance is proportional to the cleavage and oxidation of sulfonic headgroups of PFSAs, as well as carbon monoxide and carbon dioxide are thought to be generated by oxidation of the defluorinated tail and cleavage of carboxylic groups of PFCAs.

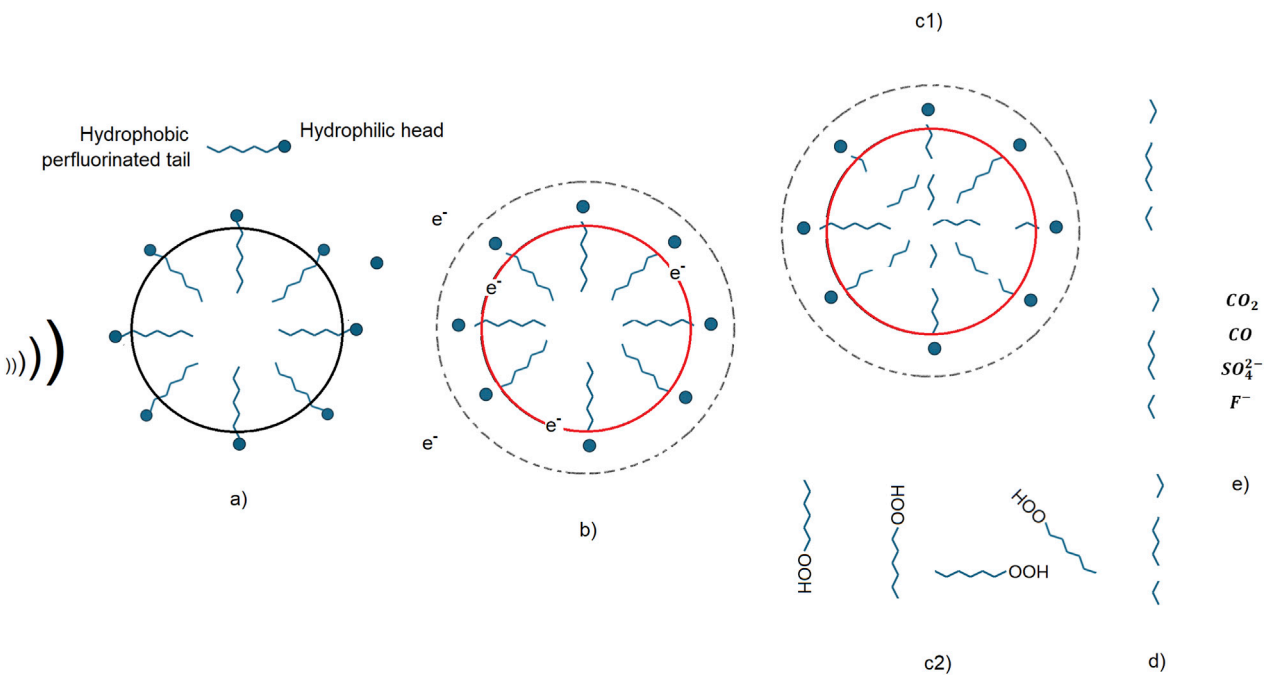

FIGURE 1
PFAS adsorption at the air-water interface **(a)**, headgroup pyrolytic cleavage upon bubble collapse **(b)**, degradation of the cleaved perfluoroalkyl chain inside the bubble **(c1)** and/or release into the liquid bulk **(c2)** followed by (a-b-c2) loop, formation of intermediates **(d)** and their hydrolysis to end products in liquid phase **(e)**.

However, sulphate head group recombination may occur, as well as CO_2 may form carbonic and formic acids, or degas from the bulk.

Concerning the concentration of fluoride ions, it may not correlate with PFAS degradation rates due to the generation of short chain or partially fluorinated products (Fernandez et al., 2016; James Wood et al., 2020; Panda et al., 2019; Rodriguez-Freire et al., 2015). Conversely, percentage fluoride release (Equation 1) can be used to define the effectiveness of the treatment (Horst et al., 2020):

$$\%F^- \, release = \frac{[F^-]}{[TOF_0]} \times 100 \quad (1)$$

Where:

$[F^-]$ = Concentration of fluoride ion (mol L^{-1}), measured by ion chromatography (James Wood et al., 2020; Lee et al., 2016) or fluoride-selective electrodes (Gole et al., 2018b; Y.-J. Lei et al., 2020);

$[TOF_0]$ = Total organic fluorine at t = 0 (mol L^{-1}), determined by combustion ion chromatography (Rodriguez-Freire et al., 2016), or from PFAS concentration at the beginning of the treatment.

Concerning sonolysis products, PFSAs can be transformed into comparable chain length PFCAs (James Wood et al., 2020; Panda et al., 2019), while the reverse is not expected when no sulphur is present. Hence, given a starting PFCA, related fluorinated by-products can be predicted by removing a CF_2 group from the original structure, and repeating until no CF_2 groups are left. Analogue approach can be used for PFSAs taking into account the cleaved chains with both SO_3H and $COOH$ headgroups (Sidnell et al., 2022).

Concentration of PFAS and degradation intermediates has been directly measured mostly by Ultra-High Performance Liquid Chromatography - Mass Spectrometry (UHPLC-MS) (Campbell et al., 2009; Cheng et al., 2010; Gole et al., 2018b; Lee et al., 2016; Y.-J. Lei et al., 2020; Lin et al., 2016; Moriwaki et al., 2005; Vecitis C. D. et al., 2008; Vecitis et al., 2010). However, predicting which by-products to measure is not always possible, especially concerning newly developed PFAS. To this aim, Total Ion Chromatogram (TIC) is a reliable tool for the identification of unknown or unexpected by-products (Gole et al., 2018b; Lee et al., 2016; Rodriguez-Freire et al., 2016).

4 Parameters affecting PFAS degradation

Degradation of PFAS by US irradiation is affected by their chemical structure and concentration, background ions, additives, co-contaminants consuming acoustic energy, pH and temperature of the solution. Process efficiency is also related to power density, ultrasonic frequency, flowrate, atmospheric condition, reactor materials and configuration. Both solution chemistry and operational conditions are discussed in this section.

4.1 Solution chemistry

Concentration is likely the most critical parameter affecting the efficiency of sonolytic treatment since it defines the rate order (Sidnell et al., 2022). Differences in functional group, chain length, and extent of fluorination influence the hydrophobicity, surface activity, and thermal activation energy of PFAS

(Fernandez et al., 2016). Oxidative additives may enhance the performance of US irradiation, which is also affected by organic matter, residual solvents, pH and temperature of the solution.

4.1.1 PFAS concentration, chemical structure and properties

Differences in the initial concentrations of PFAS correspond to different concentrations of compounds surrounding the cavitation voids, affecting the intensity of cavitation, i.e., the effectiveness of the treatment (Cao et al., 2020). There is wide evidence that the optimal rate of degradation is obtained at saturation conditions. Both defluorination and removal rates of PFOS were enhanced by rising the initial concentration of the target compound (0.32, 2.6, and 5.3 mM) during dual frequency operation in a large-scale reactor (Gole et al., 2018a). Kinetics of PFOS decomposition shifted from pseudo-first-order to zero-order by increasing PFOS concentration, as saturation of the bubble interface sites occurred (Vecitis et al., 2008a). Shende et al. (2019) draw the same conclusion on both PFOS and PFOA on the basis of the Michaelis-Menten type kinetic model developed, showing that the diffusion of these compounds at the bubble-water interface limited the mineralization rate achievable. Any increase of concentration above the optimal initial value may prevent the collapse of the voids, leading to reduced cavitation events and defluorination (Cao et al., 2020). These findings have been recently confirmed by trials on PFAS concentrated waste (Kewalramani et al., 2023).

Concerning the headgroup, the interface activity of PFCAs has been reported to be lower than that of PFSAs with analogue chain length. This has been assessed by comparison of PFOS and PFOA (Campbell and Hoffmann, 2015; Vecitis C. D. et al., 2008), PFHxA and PFHxS (Campbell et al., 2009). Conversely, degradation rates showed the opposite trend (Campbell et al., 2009; Fernandez et al., 2016; Vecitis ChadD. et al., 2008), as the headgroup speciation impacts the partitioning at the bubble–water interface. PFCAs are also defluorinated to a larger extent than PFSAs with similar chain length (Kulkarni et al., 2022; Singh Kalra et al., 2021; Xiong et al., 2023).

Degradation rates are controlled by the availability of PFAS at the ultrasonic cavity (Blotevogel et al., 2023). Accordingly, defluorination rate and degradation rates of PFCAs and PFSAs increase with the increase of the perfluoroalkyl chain length, as well as with increasing degree of fluorination, due to the related increase in hydrophobicity (Campbell and Hoffmann, 2015; Fernandez et al., 2016; Kulkarni et al., 2022). Short chain PFAS surface films are of lower stability compared to longer chain, due to their greater water solubility. Hence, short chain PFAS may desorb from the interface within the cavitating bubble lifespan (Campbell et al., 2009), i.e., prior bubble collapse. Notably, FTSAs have shown the opposite behavior. Among FTSAs of varying chain lengths (n = 4, 6, 8), 4:2 fluorotelomer sulfonate (4:2 FTS) degraded the fastest in individual solutions and in mixtures. Sonolytic rate constants correlated to diffusion coefficients, denoting that diffuse short-chain FTSAs outcompete long-chain FTSAs to adsorb and react at the bubble interface (Fagan et al., 2023).

4.1.2 Oxidative additives

Sonication at low frequencies (<100 kHz) is associated with low bubble oscillation rate, with fewer bubbles and greater in size if compared to higher frequencies (Brotchie et al., 2009; Campbell et al., 2009). Associated lower degradation rates compared to mid-high frequencies can be enhanced by the addition of chemical agents to generate oxidizing radicals, with both thermal and radical degradation mechanisms occurring to a significant extent.

The formation of cavitation bubbles during sonolysis of aqueous media results in thermolysis of water (Okitsu et al., 2006) (Equation 2). Both hydroxyl radical ($HO^{\cdot}$) and $H^{\cdot}$ have high reactivity. Hence, they can either recombine to form H_2O, H_2 and H_2O_2 (Buxton et al., 1988; Hart and Henglein, 1985; Nagata et al., 1996) (Equations 3–5, respectively) or activate several oxidative additives.

$$H_2O \overset{)))}{\rightarrow} HO^{\cdot} + H^{\cdot} \tag{2}$$

$$H^{\cdot} + HO^{\cdot} \rightarrow H_2O \tag{3}$$

$$H^{\cdot} + H^{\cdot} \rightarrow H_2 \tag{4}$$

$$HO^{\cdot} + HO^{\cdot} \rightarrow H_2O_2 \tag{5}$$

Sulfate radicals cannot act as direct oxidants in the cleavage the carbon-sulfur bond of PFSAs (Cao et al., 2020), while conflictual results are reported concerning their effect on PFCAs (Lei et al., 2020; Xiong et al., 2023). Periodate was reported to highly enhance the degradation rate of PFOA (Lee et al., 2016). Both decomposition and defluorination efficiencies of this compound have been increased by the addition of permanganate (Hu et al., 2018). The effect of sulfate, persulfate, periodate and permanganate addition is discussed in the following sections.

4.1.2.1 Sulfate and persulfate

Advanced oxidation by sulfate radicals ($SO_4^{\cdot-}$) is gaining increasing attention due to the high redox potential (E_0 = 2.5–3.1 V) and the long half-life (30–40 μs) of $SO_4^{\cdot-}$ (Hu and Long, 2016). When sulfate (SO_4^{2-}) is added, additional indirect decomposition is expected by the generation of free radicals mainly according to Equation 6 (Lin et al., 2015):

$$HO^{\cdot} + SO_4^{2-} \rightarrow OH^- + SO_4^{\cdot-} \tag{6}$$

Sulfate radicals can be also generated by persulfate ($S_2O_8^{2-}$) activation by direct US irradiation, as well as by the heat of cavitation pyrolysis (Lei et al., 2020). Activation is assumed to occur in the interfacial region, which decreases the reaction activation energy and is also conductive to further dissociation (Equations 7–9) (Wang et al., 2018).

$$S_2O_8^{2-} \overset{)))}{\rightarrow} 2SO_4^{\cdot-} \tag{7}$$

$$S_2O_8^{2-} + HO^{\cdot} \rightarrow H^+ + SO_4^{2-} + SO_4^{\cdot-} + \frac{1}{2}O_2 \tag{8}$$

$$S_2O_8^{2-} + H^{\cdot} \rightarrow H^+ + O_4^{2-} + SO_4^{\cdot-} \tag{9}$$

PFOA is known to readily adsorb onto the surfaces of the bubbles and fragmented when cavitation occurs. In the presence of sulfate radicals, additional indirect decomposition is expected. The related pathway proposed for PFOA (Lei et al., 2020), may be extended to a generic PFCA as follows. Decarboxylation reaction is initiated via cavitation pyrolysis, with associated production of perfluoroalkyl radical ($C_nF_{2n+1}^{\cdot}$) and carboxyl radical ($HOOC^{\cdot}$) (Equation 10). The attack of both these radicals by sulfate and

hydroxyl radicals results in the generation of CO_2 and $C_{n-1}F_{2n-1}COF$ (Equations 11–14). Hydrolysis of $C_{n-1}F_{2n-1}COF$ follows (Equation 15). Mineralization to CO_2 and hydrofluoric acid then proceeds via repetitive generation of short-chain intermediates (Equations 10–15 loop).

$$C_nF_{2n+1}COOH \overset{)))}{\rightarrow} C_nF_{2n+1}^{\cdot} + HOOC^{\cdot} \quad (10)$$

$$HOOC^{\cdot} + SO_4^{\cdot-} \rightarrow CO_2 + H^+ + SO_4^{2-} \quad (11)$$

$$HOOC^{\cdot} + HO^{\cdot} \rightarrow CO_2 + H_2O \quad (12)$$

$$C_nF_{2n+1}^{\cdot} + SO_4^{\cdot-} + H_2O \rightarrow C_{n-1}F_{2n-1}COF + HF + H^+ + SO_4^{2-} \quad (13)$$

$$C_nF_{2n+1}^{\cdot} + HO^{\cdot} \rightarrow C_{n-1}F_{2n-1}COF + HF \quad (14)$$

$$C_{n-1}F_{2n-1}COF + H_2O \rightarrow C_{n-1}F_{2n-1}COOH + HF \quad (15)$$

Increased degradation of PFCAs may be expected by the enhancement of decarboxylation due to the effect of sulfate radicals, which would not be able to act as direct oxidants in the cleavage the carbon-sulfur bond of PFSAs (Cao et al., 2020). Accordingly, no enhancement was observed in the decomposition of PFSAs by persulfate addition (Hori et al., 2012). The removal of PFOA - initial concentration (C_0): 120 μM - following 2 h of US irradiation at 40 kHz was observed to increase from 46% to 99% with sulfate addition (25 mM) (Lin et al., 2015). When 10 mM persulfate was used, the pseudo-first-order rate constants of perfluoroether carboxylic acids (PFECAs, C_0: 50 μM) were 2.5–3.9 times those in the absence of persulfate at 28 kHz (Hori et al., 2012). Defluorination of PFOA (C_0 = 10 μM) increased from 39.4% ± 0.8% to 100% ± 1.2% by persulfate addition (4 mM) in a dual-frequency US irradiation system at 20–43 kHz (Lei et al., 2020). Conversely, providing 1 mM of persulfate was observed to reduce the defluorination of PFOA (1.2 μM) at 20 kHz, as well as suppressed defluorination (84.54%–33.84%) was observed at increased dosage of persulfate (0.5–10 mM). Kinetics-fitted Langmuir-type adsorption modeling was provided to support that persulfate addition increases competition with PFOA for adsorption sites on the bubble-water interface, where radical oxidation and pyrolysis occur (Xiong et al., 2023). However, both the frequency and the ratio between persulfate and PFAS concentration were similar to those of a previous study reporting enhanced degradation of PFOA due to persulfate addition (Lei et al., 2020). Hence, further investigation is desired to shed light on these conflictual results.

4.1.2.2 Periodate

US-mediated activation of periodate (IO_4^-) results in the production of the free radicals $IO_3^{\cdot}$ and $IO_4^{\cdot}$ (Equations 16, 18, respectively). Production of $IO_3^{\cdot}$ is also enhanced in acidic conditions according to Equation 17 (Lee et al., 2016; Sukhatskiy et al., 2023).

$$IO_4^- \overset{)))}{\rightarrow} IO_3^{\cdot} + O^{\cdot-} \quad (16)$$

$$IO_4^- + 2H^+ \rightarrow IO_3^{\cdot} + H_2O \quad (17)$$

$$HO^{\cdot} + IO_4^- \rightarrow OH^- + IO_4^{\cdot} \quad (18)$$

Periodate addition (4.5–45 mM) in US system resulted in enhanced degradation rates of PFOA (3.25–9.25 times if compared with pure US system) at 40 kHz. As for sulfate and persulfate addition, radical reaction with PFOA, mainly driven by the radical $IO_3^{\cdot}$ (Equation 19), has been assumed to occur together with the main pyrolytic pathway (Lee et al., 2016).

$$IO_3^{\cdot} + C_nF_{2n+1}COO^- \rightarrow IO_3^- + C_nF_{2n+1}^{\cdot} + CO_2 \quad (19)$$

The resulting perfluoroalkyl free radical is then sonodegraded to C1 fluororadicals, ultimately converted into CO, CO_2, and HF (Lee et al., 2016). Further research is desired to assess the effect of periodate on different PFAS.

4.1.2.3 Permanganate

Permanganate (MnO_4^-) can be reduced by US to colloidal MnO_2 particles (Equations 20, 21) (Abulizi et al., 2014; Okitsu et al., 2009), which can serve as cavitation nucleus enhancing the effect of US cavitation by decreasing the cavitation nucleation threshold (i.e.,: enhancing pyrolytic decomposition) (Zhao et al., 2014). Moreover, oxidation in the vicinity of the MnO_2 surface is expected (Hu et al., 2018).

$$2MnO_4^- + 6H^{\cdot} \rightarrow 2MnO_2 + 2OH^- + 2H_2O \quad (20)$$

$$2MnO_4^- + 3H_2O_2 \rightarrow 2MnO_2 + 3O_2 + 2OH^- + H_2O \quad (21)$$

The catalytic potential of MnO_2 was investigated by US irradiation of PFOA (132 μM) at 40 kHz. Addition of potassium permanganate ($KMnO_4$, 10 mM) resulted in the enhancement of both decomposition and defluorination efficiencies by a factor of 2.8 and 7.2, respectively. Degradation pathway was proposed to initiate via electron extraction on the carboxylic group (Equation 22) and followed by pyrolytic cleavage of the resulting free radical (Equation 23). The formed perfluoroalkyl free radical can then be oxidized, releasing fluorine ions (Equation 24), and Equations 22–24 loop follows. Moreover, the perfluoroalkyl free radicals formed in Equations 22–24 loop can also undergo direct cleavage of the $C-C$ bonds to produce C1 fluororadicals, further oxidized to CO_2 and fluoride ions (Hu et al., 2018).

$$C_nF_{2n+1}COO^- \xrightarrow{)))\text{,MnO2}} C_nF_{2n+1}COO^{\cdot} + e^- \quad (22)$$

$$C_nF_{2n+1}COO^{\cdot} \xrightarrow{)))\text{,MnO2}} C_nF_{2n+1}^{\cdot} + CO_2 \quad (23)$$

$$C_nF_{2n+1}^{\cdot} + 2H_2O \xrightarrow{)))\text{,MnO2}} C_{n-1}F_{2n-1}COO^- + 2F^- + 4H^+ + e^- \quad (24)$$

Given the promising results reported on the degradation of PFOA, further research is recommended to investigate the effect of permanganate on different PFAS.

4.1.3 Natural dissolved organic matter

Natural dissolved organic matter (DOM) consists of a wide variety of dissolved organic molecules (Zark and Dittmar, 2018). Increased concentration of soluble fulvic acid may result in less intense cavitation (i.e., less pyrolysis of PFAS), and in reduced production of free radicals. Moreover, fulvic acid is expected to quench the free radicals produced, thereby competing with PFAS for these reactive species (Fuller et al., 2024). However, negligible effect of natural organic matter (humic and fulvic acids) has been reported on the sonolytic degradation of PFOS and PFOA in landfill groundwater (Cheng et al., 2008). Being natural organic matter surface active, minimal competitive adsorption on the bubble-water interface could be explained by the very low concentration tested

(15 mg L^{-1}). Indeed, while the addition of 0.3 g L^{-1} of soluble fulvic acid to simulated still bottoms showed no influence on the degradation rate of the studied compounds (PFHpA, PFOA, PFNA, PFHxS and PFOS), defluorination decreased from 56% to 36% and 29% when addition was increased to 3.0 and 6.1 g L^{-1}, respectively (Fuller et al., 2024).

Concerning the eventual influence of other constituents of natural DOM on the US of PFAS, their investigation may represent a potential area of future study.

4.1.4 Surfactants

Surfactants can either enhance or reduce degradation rates of PFAS sonolysis. PFOA degradation rate during ultrasonic irradiation at 40 kHz was enhanced by the use of the cationic surfactant Hexadecyl Trimethyl Ammonium Bromide (CTAB). CTAB adsorbed to the bubble-water interface, lowering surface energy and bubble coalescence, attracting PFOA, and enhancing the adsorption of the compound. Conversely, the addition of an anionic surfactant reduced the degradation rate of PFOA, due to competition for the reaction sites at the air-water interface (Lin et al., 2016). Very recently Lei et al. reported inhibited defluorination by adding surfactant directly into a polypropylene beaker containing the PFOA solution comparing to surfactant addition into the water of the US bath. SEM analysis confirmed that adsorption and wrapping between surfactant micelles and PFOA reduced the contact between PFOA and radicals and affected the surfactant effect on the surface tension (Lei et al., 2023).

The effect of surfactant concentration was assessed very recently on the degradation of PFOA, PFOS and 6:2 FTS. Dodecyltrimethylammonium chloride (DTAC, cationic), sodium dodecylbenzene sulfonate (SDBS, anionic), and Triton X-100 (TX-100, non-ionic) around critical micelle concentration inhibited PFAS degradation, likely due to the competition at the cavity bubble-water interface. However, when equal molar concentration with that of PFAS were used (low concentration range of ~0.02 mM), degradation increased. This enhancement was validated for real-world samples of aqueous film-forming foam and form fractionated waste (Awoyemi et al., 2025).

4.1.5 Residual solvents

PFAS accumulated in regenerable anion exchange resins can be removed using a salt solution, often in combination with co-solvents. The spent brine can then be effectively treated by sonication, but the solvent will likely act as a scavenger of hydroxyl radicals. Indeed, while more than 80% of PFCAs and PFSAs in artificial spent brine were degraded by US at 1,000 kHz, degradation was reduced to less than 20% by increasing methanol up to 700 g kg^{-1} (Fuller et al., 2024).

4.1.6 pH

The pH of PFAS-contaminated solution under US irradiation has been observed to become more acidic (Fernandez et al., 2016; James Wood et al., 2020; Rodriguez-Freire et al., 2016; Shende et al., 2019), due to the formation of radicals and several acid species such as HF, H_2CO_3 from dissolved CO_2, as well as HNO_2 and HNO_3 in air saturated systems (Shende et al., 2019). Further reduction of the pH has been assumed to positively charge the bubble surface (Wood et al., 2017), lowering coalescence and enhancing the affinity with hydrophobic PFAS (Gole et al., 2018a; Lee et al., 2016; Lin et al., 2015). Indeed, given their low pKa values, PFAS exist in solutions as ionized compounds, while low pH causes them to reform with hydrogen ions and adsorb to the bubble wall due to the augmented hydrophobicity (Panda et al., 2019; Price et al., 2004). At low frequencies sonication, when oxidative additives are used, the influence of pH on radical formation and destruction is mainly related to the radical-mediated degradation pathway. However, the effect of pyrolysis/plasma reactions is expected to become more significant at low pH, being the solute no more in ionic form, i.e., no more available for degradation in solution by oxidative/radical-mediated reactions (Sidnell et al., 2022).

4.1.7 Temperature

Increased temperature of the bulk water decreases the cavitation power threshold by diminishing both surface tension and viscosity, while it also enhances vaporization of the liquid matrix into the bubbles, lowering collapse temperatures (Adewuyi, 2001), gas solubility, and nucleation rates. However, being most PFAS not volatile (Buck et al., 2011), their vaporization is not likely significantly influenced by bulk temperature.

At high frequencies, where PFAS sonolysis is the main mechanism affecting PFAS degradation, PFAS degradation rates in groundwater samples increased proportionally with increasing bulk water temperature (15 °C–25 °C, at 700-kHz) (Kulkarni et al., 2022). Enhance in the rate kinetics of PFOA and PFOS was also observed at higher temperature (14.5 °C–30 °C) at frequencies between 575 kHz and 1,140 kHz (Shende et al., 2021a). At low frequencies the effect of temperature is also related to oxidative/radical-mediated reactions, i.e., to the oxidizing agents used. Major decomposition rates and defluorination were observed at the lowest temperature (25 °C–45 °C) at 40 Hz with sulfate addition (Raso et al., 1999), while PFOA decomposition and defluorination slightly increased by raising solution temperature from 30 °C to 50 °C at the same applied frequency with permanganate addition (Hu et al., 2018). The output power of ultrasonication decreases as the temperature rises under constant pressure (Raso et al., 1999), while enhanced temperature could activate PFAS oxidations by permanganate (Liu et al., 2009).

4.2 Operational conditions

Various operational parameters affect the removal efficiency of PFAS during US irradiation. Here, we discuss the effect of ultrasonic frequency, power density, flowrate, atmosphere condition, and reactor configuration.

4.2.1 US frequency

Sound frequency refers to the number of periodic oscillations per second (Clark, 2001). In a US system, frequency affects number, size distribution, symmetry, oscillation rate and lifespan of the bubbles, collapse intensity of cavitation events, ratio of standing/travelling waves, and formation of free radicals (Brotchie et al., 2009; Pflieger et al., 2019; Shende et al., 2021a; Suslick, 1989). To compare frequency effects, power must be carefully controlled (Sidnell et al., 2022).

Low US frequencies produce large bubbles, and higher individual collapse temperatures, compared to higher frequencies.

At high ultrasonic frequencies, acoustic bubbles reach the resonance size and collapse in a very short time. As a result, the resonant size of the bubbles reduces, as well as the frequency of cavitation events increases. High population of bubbles with average small size increases the number of active sites at the interface available for adsorption, i.e., the mass of solute which can move from the bulk to the cavitation bubble interface to be decomposed by interfacial pyrolysis (Campbell et al., 2009; Cao et al., 2020; Petrier and Francony, 1997). Accordingly, at low frequencies (20–100 kHz), reaction rates of PFAS degradation are lower if compared to mid-high frequency sonication (100–1,000 kHz), especially if no oxidative agents are provided (Sidnell et al., 2022). Most PFAS are fully mineralized by US irradiation at mid-high frequencies (Campbell et al., 2009; James Wood et al., 2020; Lee et al., 2016; Moriwaki et al., 2005), due to increased generation of bubbles, radicals formation and surface availability. However, degradation rates decrease at frequencies >1,000 kHz (Campbell et al., 2009; James Wood et al., 2020), due to the reduced thinning and compression periods of US wave (Cao et al., 2020). Hence, a balance between cavity population and collapse intensity is required for environmental remediation.

Several works were carried out with the aim of identifying the optimum sonication frequency. US irradiation of PFOA, PFOS and HFPO-DA has been carried out at four applied frequencies (375, 580, 860 and 1,140 kHz). The frequency of 580 kHz was associated with the highest degradation of all the compounds tested, at all power density applied (200, 300, and 400 W L^{-1}) (Ilić et al., 2023). In a separate study investigating applied frequencies among 202 and 1,060 kHz at a constant power density of 250 W L^{-1} sonolysis rate constants of PFOS and PFOA have been observed to peak at 358 kHz. Notably, the highest degradation of PFBA and PFBS occurred at 610 kHz. Hence, short chains PFAS required higher frequencies to enhance the mass transfer to the bubble-water interface, compared to the analogue longer chain (Campbell et al., 2009).

Concerning dual frequency sonolysis, the aim of coupling different frequencies is to generate enhanced response from oscillating bubbles that are multiple of the natural frequency. Single sinusoidal waves exert an equal driving effort in rarefaction and compression, while the related bubble collapse time is considerably shorter than the expansion phase. By the optimal coupling of two different frequencies, the waveform spends most of its effort in rarefaction. Hence, bubbles maximize their size, before a rapid compression (Campbell and Hoffmann, 2015). PFAS pseudo-first order rate constants observed at 202 kHz were increased by 23% (PFOA) and 12% (PFOS) by adding the 20 kHz horn. Conversely, no enhancement was observed compared to degradation at 610 kHz combined with 20 kHz compared with 610 kHz alone. This was explained assuming the amplitude of the acoustic field as related to the fundamental and second-harmonic, according to Equation 25 (Kawabata and Umemura, 1996):

$$P_a(r,t) = a_1(r)\sin\left(\omega t + \phi_1(r)\right) + a_2(r)\left[\sin\left(2\left(\omega t + \phi_1(r)\right)\right) + \Delta\phi(r)\right] \quad (25)$$

where $P_a(r,t)$ is the acoustic pressure at point r at time t and $a_1(r)$ and $a_2(r)$ are the amplitudes of the fundamental and the second harmonic at point r, respectively. ω is the angular frequency of the fundamental, $\phi_1(r)$ the phase of the fundamental at point r, and $\Delta\phi(r)$ the phase of the second harmonic relative to the fundamental. The second harmonic superimposition is sensitive to the relative phase $\Delta\phi$, i.e., enhanced cavitation and induction of sonochemical reactions arise from the synergy between the acoustic waveforms, rather than from the sum of independent effects. Hence, the US frequency of 20 + 202 kHz led to improved overlap of waveforms compared to 20 + 610 kHz exposure, with resulting enhanced sonochemical effects (Campbell and Hoffmann, 2015).

In summary, PFAS sonolysis is most effective at middle frequencies (100–1,000 Hz), while low frequencies require oxidative additives. Further investigation is desired to assess the promising synergy arising from the proper coupling of different frequencies.

4.2.2 Power density

Power density defines the energy input in a US system (Cao et al., 2020). Enhancing US power can improve PFAS degradation by increasing the population, size, collapse temperature and pressure of active voids (Wood et al., 2017; Zhou et al., 2013). Enhanced production of radicals (Mason, 2000), mixing of the solution, and stabilization of bubbles at the wave antinodes (Matula, 1999) are also expected. Further increase in power above a specific level reduces reaction rates. Several phenomena may concur with this reduction. A high population of bubbles in the treated media may scatter the US wave to the inner surface of the reactor or back to the transducers (Thompson et al., 2011), as well as agglomerates of bubbles grown on the surface of the emitter may scatter the US waves and lead to their decay (Suslick et al., 1999; Thompson et al., 2011). Moreover, large bubbles may lose their effectiveness due to reduced collapse temperature and pressure (Gogate and Pandit, 2000; Shin-ichi Hatanaka et al., 2001; Sunartio et al., 2005). Lastly, increased population of bubbles increased in size may result in bubble expulsion from the sonochemically active antinode regions and degas from the solution (Shin-ichi Hatanaka et al., 2001).

The effect of increasing power density has been investigated on several PFAS, at different applied frequencies. Simultaneous sonication of PFOA (240 nM) and PFOS (200 nM) showed a linear increase of the degradation rates of both compounds at 358 kHz and 610 kHz (Campbell and Hoffmann, 2015). Similar results have been obtained in a separate study at 575 kHz, where pseudo-first-order degradation kinetics have been observed for PFOA and PFOS (100–150 nM each) at increasing power densities (30 W L^{-1}–262 W L^{-1}) with and without sparging Argon (Shende et al., 2021b). Near-linear increase of the degradation rates has been also observed during the simultaneous sonication of PFHxA (320 nM) and PFHxS (230 nM) at 202 kHz, while degradation rate of PFHxA peaked at 250 W L^{-1} at 610 kHz. US irradiation of PFBA (470 nm) and PFBS (300 nm) show an increase of degradation rates at 610 kHz, while both peaked at 250 W L^{-1} at 202 kHz (Campbell and Hoffmann, 2015). Very recently, degradation kinetics of HFPO-DA (1 mg L^{-1}) have also been investigated at different power densities (200–400 W L^{-1}). Degradation performance increased consistently with increasing power density at all the frequencies tested (375, 580, 860 and 1,140 kHz) (Ilić et al., 2023).

Compared to the mid-high sonication frequencies and the initial concentrations here discussed, much higher power density

(3750 W L^{-1}) was required to observe the degradation peak of trace level (200 pM) of PFOA and PFOS at 20 kHz (Panda et al., 2019).

4.2.3 Flowrate

Notwithstanding flowrate of the treated solution through a US reactor may affect the size, shape, and spatial distribution of ultrasonic cavities (Sidnell et al., 2023), there is lack of investigation in this regard.

The effect of increasing recirculation rates (0–889 min^{-1}) was investigated on the US degradation of PFOS (200 W L^{-1}, 410 kHz, 30 min) and compared with measured KI dosimetry, calorimetry, sonoluminescence, and sonochemiluminescence (Sidnell et al., 2023). Recirculation enhanced defluorination up to 14% at flowrates of 79 and 214 mL min^{-1}. Flowrates which increased defluorination correlated slightly with enhanced sonochemiluminescence and negatively affected sonoluminescence, calorimetry, and dosimetry. Effects were attributed to perturbation of the bubble walls, causing asymmetric cavity collapse, and eventually enhanced solvated electron production/interaction. Further increase of the flowrate resulted in sonochemical measurements similar to those obtained without flow, as a consequence of continued collapse temperature quenching by furthered bubble asymmetry. Effects at 79 and 214 mL min^{-1} were most relevant in the very beginning of the treatment, suggesting a dynamic bubble size distribution which stabilized after ~15 min. However, these results indicate that optimization of the flowrate could reduce treatment times compared to both batch systems and non-optimized flow systems. Moreover, providing flowrate significantly contributed to reactor cooling. Thus, optimization of the flowrate would likely reduce operating time and costs at full scale (Sidnell et al., 2023).

4.2.4 Atmosphere condition

Solubility, thermal conductivity, and polytropic index (which relates pressure to volume) of the dissolved gases may affect the bubble temperature and the effectiveness of cavitation (Henglein, 1987; Neppiras, 1980).

The effect of various gases (helium, nitrogen, argon, oxygen, and ozone) was investigated during US of a mixture of PFOA (102 nM) and PFOS (113 nM) (575 kHz, 77 W L^{-1}, 2 h). Higher degradation rates were observed without sparging any gas (i.e., in air environment). Unstable cavities form in a solution having a high dissolved concentration of gases (Brenner et al., 1996; Rooze et al., 2013). Hence, considering that experiments were carried out in a fully saturated gas environment, the authors proposed that a higher number of unstable cavities might have formed, lowering the rate of PFAS degradation (Shende et al., 2021a). However, previous US trials (200 kHz, 3.33 kW L^{-1}, 60 min) reported a great enhancement of degradation rates of PFOA and PFOS (single solutions, 10 mg L^{-1} each) in solutions saturated with argon gas (from 0.0155 to 0.032 min^{-1}, and from 0.0068 to 0.016 min^{-1}, respectively), compared with air environment. This was in agreement with the polytropic index (γ) of the gases ($\gamma_{argon} > \gamma_{air}$) (Moriwaki et al., 2005). Indeed, being the highest temperature in the cavitating bubble (T_{max}) defined according to Equation 26, a higher γ produces a higher temperature, leading to enhanced reaction yield (Okitsu et al., 2006).

$$T\,\max = T_{in}\left[P_a\left(\gamma - 1\right)/P_{in}\right] \tag{26}$$

where T_{in} is the initial temperature in the bubble; P_{in} the initial pressure; P_a is the acoustic pressure when collapse begins; γ is the ratio of the specific heat at constant pressure to the specific heat at constant volume of the gas into the bubble (Nagata et al., 2000).

Concerning US irradiation at low frequency, sonochemical effects of differing dissolved gases relate also to chemical effects. During periodate-assisted treatment of PFOA at 40 kHz the rate of degradation increased with reduced dissolved oxygen concentration under nitrogen, air, and oxygen atmosphere. Oxygen was assumed to reduce the total amount of effective free radicals $IO_3^{\cdot}$ (Lee et al., 2016). Argon atmosphere increased degradation and defluorination of PFOA also in a permanganate-US system. Here, enhanced performance was linked to high collapse temperature and radical production rate (Hu et al., 2018).

4.2.5 Reactor configuration

Very recently, optimization of reactor configuration was investigated by varying reactor volume and height of the bulk (0.6–1.4 L; 5.7–34.0 cm, respectively), power density (100–350 W L^{-1}), and number of modular reactors (1–3), for the US irradiation of PFOS (C_0: 10.0 mg L^{-1}). Peak of the defluorination rate (3.40 μmol L^{-1} min^{-1}) occurred at 14.2 cm, in the 0.6 L reactor, under 200 W L^{-1} applied power density, while increasing the number of transducers connected in parallel to one amplifier enhanced process efficiency from 78.6 to 191.8 μmol kWh^{-1} (Sidnell et al., 2024).

The effect of different reactor materials was also recently investigated (Khoshyan et al., 2024). Materials with high stiffness generally show reduced intermolecular distance. Hence, the propagation of sound waves is facilitated by enhanced transmission of kinetic energy vibrations along strengthened intermolecular connections, i.e.,: higher sound velocity is expected in hard materials compared to soft ones (Angelskår et al., 2019; Lochab and Singh, 2004). Approximately 95% and 46% defluorination of PFOA (1 mg L^{-1}) was achieved in a glass reactor and in a polypropylene reactor, respectively (130 kHz, 50–55 W L^{-1}, 3 h). Superior defluorination was also achieved in the glass reactor when treating PFOS, 6:2 FTS, and aqueous film-forming foam containing a complex mixture of PFAS, confirming that glass exhibits significantly higher efficiency in US irradiation transportation (Khoshyan et al., 2024).

Notably, future reactor design may also evaluate controlled atmosphere-configurations. Indeed, a very recent monitoring of US applied to spent brine from regenerable exchange resins detected significant quantities of volatile organic fluorine species (Fuller et al., 2024).

5 Combination with other techniques

Synergy among different remediation techniques can be accomplished either by consecutive approaches (i.e., PFAS removal and destruction), or by their simultaneous application (Figure 2). Concerning consecutive approaches, activated carbon, ion exchange resins and silicas are applied in water treatment to remove PFAS. US can be used to destroy the PFAS load of the solvent used for the regeneration of the sorbents (Uriakhil et al., 2021). Low power-US was also directly applied on modified granular

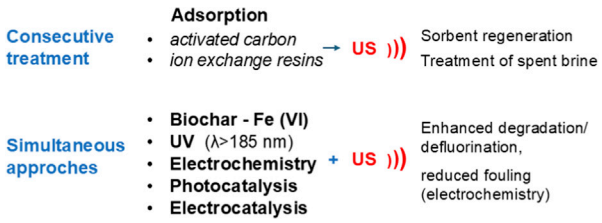

FIGURE 2
Combination of US with other techniques: consecutive and simultaneous approaches for PFAS treatment.

activated carbon to enhance the desorption of PFAS, with minimum disruption of the adsorbent's structure, and a negligible decrease in the sorbent's capacity over four saturation rounds (Ramos et al., 2022). Concerning regenerable ion exchange resins, significant mineralization of PFAS in spent brine and still bottoms was achieved at 1,000 kHz (Fuller et al., 2024).

Simultaneous approaches have been investigated with sorbents, UV, electrochemical treatment, photo- and electrocatalysis. Very recently a US/biochar/Fe (VI) system achieved 93% PFOA defluorination, compared with 28% and 49% by US/biochar and US/Fe (VI), respectively, implying strong synergistic effect (Lei et al., 2024). Regarding the application of UV, the photon energy of UV radiation with a wavelength of 185 nm (647 kJ mol^{-1}) overcomes the binding energy of the C-F bond (452 kJ mol^{-1}) (Merino et al., 2016). Hence, high energy photons can degrade PFAS. Simultaneous application of UV (2 lamps, 8 W, λ = 185 nm) and US (600 kHz) was tested for the degradation of PFOS (10 mg L^{-1}). Compared with US alone, UV-assisted US irradiation enhanced defluorination (+12.01%) and degradation (+8.76%) rates of PFOS within 6 h (Yang et al., 2013). Later, Sekiguchi et al. investigated UV radiation (2 lamps, 6.3 W, λ = 254 nm with 3% output power at 185 nm) and US (200 kHz,100 W L^{-1}) on the degradation of PFOA and PFPrA (100 ppm each). Under the UV, US, and US + UV conditions, 2.72%, 8.25%, and 12.2% of PFOA was defluorinated, respectively, within 2 h, while defluorination ratios of PFPrA were 2.18%, 6.12%, and 9.28% under US, UV, and US + UV conditions, respectively (Sekiguchi et al., 2017).

Concerning the coupling of US with electrochemical degradation, total PFOA (50 μM) disappearance and 43% defluorination were obtained within 6 h by a stainless steel/ Ti_4O_7/stainless steel electrode configuration, at 50 mA cm^2, and Na_2SO_4 0.15 M as supporting electrolyte. US alone at 130 kHz achieved only 33.3% PFOA removal and 5.6% defluorination, but when applied simultaneously with the electrochemical treatment, complete PFOA degradation was accompanied by enhanced defluorination (63.5%). The synergy of the combination resulted in activated/cleaned electrode surface, improved mass transfer, and enhanced production of radicals (Luo et al., 2023). Even the photocatalytic decomposition (TiO_2, 16 W UV mercury lamp, λ = 254 nm) of PFOA (120 μM) increased from 22% to 45% within 7 h by coupling US irradiation at 40 kHz. US enhanced the treatment efficiency by improving the physical dispersion and mass transfer at the TiO_2 surface (Panchangam et al., 2009).

Regarding the simultaneous application of electrocatalysis and US, a very recent investigation showed promising results (Wang et al., 2024). Polytetrafluoroethylene (PTFE) particles (1–5 μm) have been used as catalyst and low frequency US (40 kHz) was coupled for activation. The system achieved near-complete defluorination of various PFAS. The underlying mechanism has been proposed by the authors as follows. Contact electrification among PTFE and water, which induces cumulative electrons on PTFE surface, results in a high surface voltage. Abundant reactive oxygen species and a strong interfacial electrostatic field are generated, the latter activating PFAS molecules, and reducing the energy barrier of O_2^- nucleophilic reaction. The simultaneous presence of surface electrons and hydroxyl radicals ultimately results in synergetic reduction and oxidation of PFAS and related intermediates (Wang et al., 2024).

Consecutive and simultaneous approaches have shown promising results. Further investigation is encouraged, as they may offer a viable option to enhance the scalability of sonolysis with the view of the implementation of this technology in full-scale treatment facilities.

6 Conclusion

Propagation of US in contaminated aqueous media results in sonophysical and sonochemical effects, able to collaboratively mineralize most of PFAS at mid-high frequencies, while oxidative additives are required to increase the rate of degradation at low frequencies. Additional research is desired to clarify the effect of sulfate and persulfate on PFCAs, as well as on the addition of periodate, given the significant enhancement reported in the degradation rate of PFOA. PFAS concentration is a critical factor affecting sonolytic treatment efficiency, since it defines the rate order. Differences in functional group, chain length, and extent of fluorination influence hydrophobicity, surface activity, and thermal activation energy of PFAS. Background water constituents and co-contaminants add further complexity. Concerning frequency and power of operation, a balance between cavity population and collapse intensity is required for environmental remediation. Further research is desired to assess the influence of pH and temperature. The effect of solution chemistry and operational conditions still needs to be validated on a broad range of compounds.

Sonolysis of PFAS has been investigated mostly under controlled lab settings. Scaling up the technique for viable PFAS treatment faces hurdles, which can be overcome by advancing reactor design and optimizing operational conditions, taking into account the specific

solution chemistry of the media demanding remediation. Pilot-scale investigations are required to evaluate scale-up and maintenance of the technology. Moreover, energy consumption is a decisive factor that demands further investigation. To this aim, optimization of the flowrate is recommended. Accomplishing synergy among different remediation techniques, either by consecutive approaches, or by their simultaneous application, may be the key approach towards the large-scale implementation of US to achieve full and efficient PFAS mineralization.

Author contributions

AT: Investigation, Writing – review and editing, Methodology, Data curation, Writing – original draft, Conceptualization, Formal Analysis. JU: Writing – review and editing. MP: Conceptualization, Writing – review and editing. JK: Funding acquisition, Writing – review and editing, Conceptualization. IC: Conceptualization, Writing – review and editing, Funding acquisition.

Funding

The author(s) declared that financial support was received for this work and/or its publication. The study was funded by Formas, the Swedish Research Council for Environment, Agricultural Sciences and Spatial Planning, within the National Research Programme for Seas and Water, case number 2023-01974, as well as by the J.C. Kempe and Seth M. Kempe Memorial Foundations (Kempestiftelserna).

Conflict of interest

The author(s) declared that this work was conducted in the absence of any commercial or financial relationships that could be construed as a potential conflict of interest.

Generative AI statement

The author(s) declared that generative AI was not used in the creation of this manuscript.

Any alternative text (alt text) provided alongside figures in this article has been generated by Frontiers with the support of artificial intelligence and reasonable efforts have been made to ensure accuracy, including review by the authors wherever possible. If you identify any issues, please contact us.

Publisher's note

References

Abulizi, A., Yang, G. H., Okitsu, K., and Zhu, J. J. (2014). Synthesis of MnO2 nanoparticles from sonochemical reduction of MnO4– in water under different pH conditions. *Ultrason. Sonochem* 21, 1629–1634. doi:10.1016/J.ULTSONCH.2014.03.030

Adewuyi, Y. G. (2001). Sonochemistry: environmental science and engineering applications. *Ind. Eng. Chem. Res.* 40, 4681–4715. doi:10.1021/IE010096L

Angelskår, H., Dirdal, C. A., Tronstad, T. V., Kavli, T., and Vogl, A. (2019). Low-loss ultrasound transmission through glass assisted by resonance. *Ultrasonics* 96, 160–164. doi:10.1016/J.ULTRAS.2019.01.011

Asadi Zeidabadi, F., Banayan Esfahani, E., Moreira, R., McBeath, S. T., Foster, J., and Mohseni, M. (2024). Structural dependence of PFAS oxidation in a boron doped diamond-electrochemical system. *Environ. Res.* 246, 118103. doi:10.1016/j.envres.2024.118103

Awoyemi, O. S., Naidu, R., and Fang, C. (2025). Surfactant-assisted ultrasonic degradation of per- and polyfluoroalkyl substances (PFAS): effect of surfactant concentration. *J. Clean. Prod.* 519, 146042. doi:10.1016/J.JCLEPRO.2025.146042

Blotevogel, J., Thagard, S. M., and Mahendra, S. (2023). Scaling up water treatment technologies for PFAS destruction: current status and potential for fit-for-purpose application. *Curr. Opin. Chem. Eng.* 41, 100944. doi:10.1016/j.coche.2023.100944

Brenner, M. P., Hilgenfeldt, S., and Lohse, D. (1996). Why air bubbles in water glow so easily. *Nonlinear Phys. Complex Syst.*, 79–97. doi:10.1007/BFB0105431

Brotchie, A., Grieser, F., and Ashokkumar, M. (2009). Effect of power and frequency on bubble-size distributions in Acoustic cavitation. *Phys. Rev. Lett.* 102, 084302. doi:10.1103/PhysRevLett.102.084302

Buck, R. C., Franklin, J., Berger, U., Conder, J. M., Cousins, I. T., Voogt, P.De, et al. (2011). Perfluoroalkyl and polyfluoroalkyl substances in the environment: terminology, classification, and origins. *Integr. Environ. Assess. Manag.* 7, 513–541. doi:10.1002/IEAM.258

Buxton, G. V., Greenstock, C. L., Helman, W. P., and Ross, A. B. (1988). Critical review of rate constants for reactions of hydrated electrons, hydrogen atoms and hydroxyl radicals·OH/·O– in aqueous Solution. *J. Phys. Chem. Ref. Data* 17, 513–886. doi:10.1063/1.555805

Campbell, T., and Hoffmann, M. R. (2015). Sonochemical degradation of perfluorinated surfactants: power and multiple frequency effects. *Sep. Purif. Technol.* 156, 1019–1027. doi:10.1016/j.seppur.2015.09.053

Campbell, T. Y., Vecitis, C. D., Mader, B. T., and Hoffmann, M. R. (2009). Perfluorinated surfactant chain-length effects on sonochemical kinetics. *J. Phys. Chem. A* 113, 9834–9842. doi:10.1021/jp903003w

Cao, H., Zhang, W., Wang, C., and Liang, Y. (2020). Sonochemical degradation of poly- and perfluoroalkyl substances – a review. *Ultrason. Sonochem* 69, 105245. doi:10.1016/j.ultsonch.2020.105245

Cheng, J., Vecitis, C. D., Park, H., Mader, B. T., and Hoffmann, M. R. (2008). Sonochemical degradation of perfluorooctane sulfonate (PFOS) and perfluorooctanoate (PFOA) in landfill groundwater: environmental matrix effects. *Environ. Sci. Technol.* 42, 8057–8063. doi:10.1021/es8013858

Cheng, J., Vecitis, C. D., Park, H., Mader, B. T., and Hoffmann, M. R. (2010). Sonochemical degradation of Perfluorooctane sulfonate (PFOS) and perfluorooctanoate (PFOA) in groundwater: kinetic effects of matrix inorganics. *Environ. Sci. Technol.* 44, 445–450. doi:10.1021/es902651g

Clark, W. W. (2001). "Noise and ultrasound," in *Patty's toxicology* (Wiley). doi:10.1002/0471435139.tox099

Das, S., and Ronen, A. (2022). A review on removal and destruction of Per- and Polyfluoroalkyl Substances (PFAS) by novel membranes. *Membr. (Basel)* 12, 662. doi:10.3390/membranes12070662

Fagan, W. P., Thayer, S. R., and Weavers, L. K. (2023). Kinetics and mechanism of ultrasonic defluorination of fluorotelomer sulfonates. *J. Phys. Chem. A* 127, 6309–6319. doi:10.1021/acs.jpca.3c03011

Fernandez, N. A., Rodriguez-Freire, L., Keswani, M., and Sierra-Alvarez, R. (2016). Effect of chemical structure on the sonochemical degradation of perfluoroalkyl and polyfluoroalkyl substances (PFASs). *Environ. Sci. (Camb)* 2, 975–983. doi:10.1039/C6EW00150E

Fuller, M. E., Zhao, Y., Hedman, P. C., Koster van Groos, P. G., Soto, A., Boodoo, F., et al. (2024). Sonochemical degradation of PFAS in ion exchange regeneration wastes. *J. Hazard Mater* 471, 134291. doi:10.1016/j.jhazmat.2024.134291

Gogate, P. R., and Pandit, A. B. (2000). Engineering design method for cavitational reactors: I. Sonochemical reactors. *AIChE J.* 46, 372–379. doi:10.1002/AIC.690460215

Gole, V. L., Fishgold, A., Sierra-Alvarez, R., Deymier, P., and Keswani, M. (2018a). Treatment of perfluorooctane sulfonic acid (PFOS) using a large-scale sonochemical reactor. *Sep. Purif. Technol.* 194, 104–110. doi:10.1016/j.seppur.2017.11.009

Gole, V. L., Sierra-Alvarez, R., Peng, H., Giesy, J. P., Deymier, P., and Keswani, M. (2018b). Sono-chemical treatment of per- and poly-fluoroalkyl compounds in aqueous film-forming foams by use of a large-scale multi-transducer dual-frequency based acoustic reactor. *Ultrason. Sonochem* 45, 213–222. doi:10.1016/j.ultsonch.2018.02.014

Hart, E. J., and Henglein, A. (1985). Free radical and free atom reactions in the sonolysis of aqueous iodide and formate solutions. *J. Phys. Chem.* 89, 4342–4347. doi:10.1021/j100266a038

Henglein, A. (1987). Sonochemistry: historical developments and modern aspects. *Ultrasonics* 25 (1), 6–16. doi:10.1016/0041-624X(87)90003-5

Hori, H., Nagano, Y., Murayama, M., Koike, K., and Kutsuna, S. (2012). Efficient decomposition of perfluoroether carboxylic acids in water with a combination of persulfate oxidant and ultrasonic irradiation. *J. Fluor Chem.* 141, 5–10. doi:10.1016/J.JFLUCHEM.2012.05.012

Horst, J., McDonough, J., Ross, I., and Houtz, E. (2020). Understanding and managing the potential by-products of PFAS destruction. *Groundw. Monit. and Remediat.* 40, 17–27. doi:10.1111/gwmr.12372

Hu, P., and Long, M. (2016). Cobalt-catalyzed sulfate radical-based advanced oxidation: a review on heterogeneous catalysts and applications. *Appl. Catal. B* 181, 103–117. doi:10.1016/J.APCATB.2015.07.024

Hu, Y., Lo, S.-L., Li, Y.-F., Lee, Y.-C., Chen, M.-J., and Lin, J.-C. (2018). Autocatalytic degradation of perfluorooctanoic acid in a permanganate-ultrasonic system. *Water Res.* 140, 148–157. doi:10.1016/j.watres.2018.04.044

Ilić, N., Andalib, A., Lippert, T., Knoop, O., Franke, M., Bräutigam, P., et al. (2023). Ultrasonic degradation of GenX (HFPO-DA) – performance comparison to PFOA and PFOS at high frequencies. *Chem. Eng. J.* 472, 144630. doi:10.1016/j.cej.2023.144630

James Wood, R., Sidnell, T., Ross, I., McDonough, J., Lee, J., and Bussemaker, M. J. (2020). Ultrasonic degradation of perfluorooctane sulfonic acid (PFOS) correlated with sonochemical and sonoluminescence characterisation. *Ultrason. Sonochem* 68, 105196. doi:10.1016/j.ultsonch.2020.105196

Karatas, O., Khataee, A., Kobya, M., and Yoon, Y. (2023). Electrochemical oxidation of perfluorooctanesulfonate (PFOS) from simulated soil leachate and landfill leachate concentrate. *J. Water Process Eng.* 56, 104292. doi:10.1016/j.jwpe.2023.104292

Kawabata, K., and Umemura, S. (1996). Use of second-harmonic superimposition to induce chemical effects of ultrasound. *J. Phys. Chem.* 100, 18784–18789. doi:10.1021/jp962137a

Kewalramani, J. A., Marsh, R. W., Prajapati, D., and Meegoda, J. N. (2023). Kinetics effects of the power density and initial concentration on the sonochemical degradation of PFOS and PFOA in concentrated waste. *J. Water Process Eng.* 53, 103752. doi:10.1016/j.jwpe.2023.103752

Khoshyan, A., Luo, Y., Nolan, A., Megharaj, M., Naidu, R., and Fang, C. (2024). Degradation of per- and poly-fluoroalkyl substances (PFAS) using ultrasonication: effect of reactor materials. *J. Water Process Eng.* 63, 105511. doi:10.1016/j.jwpe.2024.105511

Kulkarni, P. R., Richardson, S. D., Nzeribe, B. N., Adamson, D. T., Kalra, S. S., Mahendra, S., et al. (2022). Field demonstration of a sonolysis reactor for treatment of PFAS-Contaminated groundwater. *J. Environ. Eng.* 148, 06022005. doi:10.1061/(ASCE)EE.1943-7870.0002064

Lauterborn, W., and Mettin, R. (2023). "Acoustic cavitation: bubble dynamics in high-power ultrasonic fields," in *Power ultrasonics: applications of high-intensity ultrasound*. doi:10.1016/B978-0-12-820254-8.00005-1

Lee, Y.-C., Chen, M.-J., Huang, C.-P., Kuo, J., and Lo, S.-L. (2016). Efficient sonochemical degradation of perfluorooctanoic acid using periodate. *Ultrason. Sonochem* 31, 499–505. doi:10.1016/j.ultsonch.2016.01.030

Lei, Y.-J., Tian, Y., Sobhani, Z., Naidu, R., and Fang, C. (2020). Synergistic degradation of PFAS in water and soil by dual-frequency ultrasonic activated persulfate. *Chem. Eng. J.* 388, 124215. doi:10.1016/j.cej.2020.124215

Lei, Y., Zhao, L., Fang, C., Naidu, R., Tian, D., Zhao, L., et al. (2023). A novel enhanced defluorination of perfluorooctanoic acids by surfactant-assisted ultrasound coupling persulfate. *Sep. Purif. Technol.* 317, 123906. doi:10.1016/j.seppur.2023.123906

Lei, Y., Pu, R., Tian, Y., Wang, R., Naidu, R., Deng, S., et al. (2024). Novel enhanced defluorination of perfluorooctanoic acids by biochar-assisted ultrasound coupling ferrate: performance and mechanism. *Bioresour. Technol.* 402, 130790. doi:10.1016/j.biortech.2024.130790

Lenka, S. P., Kah, M., and Padhye, L. P. (2021). A review of the occurrence, transformation, and removal of poly- and perfluoroalkyl substances (PFAS) in wastewater treatment plants. *Water Res.* 199, 117187. doi:10.1016/j.watres.2021.117187

Li, Z., Huang, H.-H., Huang, Y., Huang, J., Shen, M., Zheng, J., et al. (2023). Highly efficient electrochemical oxidation of hexafluoropropylene oxide homologues at a boron-doped diamond anode. *J. Environ. Chem. Eng.* 11, 109280. doi:10.1016/j.jece.2023.109280

Lin, J.-C., Lo, S.-L., Hu, C.-Y., Lee, Y.-C., and Kuo, J. (2015). Enhanced sonochemical degradation of perfluorooctanoic acid by sulfate ions. *Ultrason. Sonochem* 22, 542–547. doi:10.1016/j.ultsonch.2014.06.006

Lin, J. C., Hu, C. Y., and Lo, S. L. (2016). Effect of surfactants on the degradation of perfluorooctanoic acid (PFOA) by ultrasonic (US) treatment. *Ultrason. Sonochem* 28, 130–135. doi:10.1016/J.ULTSONCH.2015.07.007

Liu, C., Qiang, Z., Adams, C., Tian, F., and Zhang, T. (2009). Kinetics and mechanism for degradation of dichlorvos by permanganate in drinking water treatment. *Water Res.* 43, 3435–3442. doi:10.1016/J.WATRES.2009.05.001

Lochab, J., and Singh, V. R. (2004). Acoustic behaviour of plastics for medical applications. *IJPAP* 42, 595–599.

Luo, Y., Khoshyan, A., Al Amin, M., Nolan, A., Robinson, F., Fenstermacher, J., et al. (2023). Ultrasound-enhanced Magnéli phase Ti4O7 anodic oxidation of per- and polyfluoroalkyl substances (PFAS) towards remediation of aqueous film forming foams (AFFF). *Sci. Total Environ.* 862, 160836. doi:10.1016/j.scitotenv.2022.160836

Marín-Marín, M. L., Rubio-Clemente, A., and Peñuela, G. (2023). Advanced oxidation processes used in the treatment of perfluoroalkylated substances in water. *Rev. UIS Ing.* 22, 135–150. doi:10.18273/revuin.v22n3-2023010

Mason, T. J. (2000). Large scale sonochemical processing: aspiration and actuality. *Ultrason. Sonochem* 7, 145–149. doi:10.1016/S1350-4177(99)00041-3

Matula, T. J. (1999). Inertial cavitation and single–bubble sonoluminescence. *Philosophical Trans. R. Soc. Lond. Ser. A Math. Phys. Eng. Sci.* 357, 225–249. doi:10.1098/RSTA.1999.0325

Merino, N., Qu, Y., Deeb, R. A., Hawley, E. L., Hoffmann, M. R., and Mahendra, S. (2016). Degradation and removal methods for Perfluoroalkyl and polyfluoroalkyl substances in water. *Environ. Eng. Sci.* 33, 615–649. doi:10.1089/ees.2016.0233

Mirabediny, M., Sun, J., Yu, T. T., Åkermark, B., Das, B., and Kumar, N. (2023). Effective PFAS degradation by electrochemical oxidation methods-recent progress and requirement. *Chemosphere* 321, 138109. doi:10.1016/j.chemosphere.2023.138109

Moriwaki, H., Takagi, Y., Tanaka, M., Tsuruho, K., Okitsu, K., and Maeda, Y. (2005). Sonochemical decomposition of perfluorooctane sulfonate and perfluorooctanoic acid. *Environ. Sci. Technol.* 39, 3388–3392. doi:10.1021/es040342v

Nagata, Y., Hirai, K., Bandow, H., and Kimaeda, Y. (1996). Decomposition of hydroxybenzoic and humic acids in water by ultrasonic irradiation. *Environ. Sci. Technol.* 30 (4), 1133–1138. doi:10.1021/es950336m

Nagata, Y., Nakagawa, M., Okuno, H., Mizukoshi, Y., Yim, B., and Maeda, Y. (2000). Sonochemical degradation of chlorophenols in water. *Ultrason. Sonochem* 7, 115–120. doi:10.1016/S1350-4177(99)00039-5

Neppiras, E. A. (1980). Acoustic cavitation. *Phys. Rep.* 61 (Issue 3), 159–251. doi:10.1016/0370-1573(80)90115-5

Okitsu, K., Suzuki, T., Takenaka, N., Bandow, H., Nishimura, R., and Maeda, Y. (2006). Acoustic multibubble cavitation in water: a new aspect of the effect of a rare gas atmosphere on bubble temperature and its relevance to sonochemistry. *J. Phys. Chem. B* 110, 20081–20084. doi:10.1021/jp064598u

Okitsu, K., Iwatani, M., Nanzai, B., Nishimura, R., and Maeda, Y. (2009). Sonochemical reduction of permanganate to manganese dioxide: the effects of H2O2 formed in the sonolysis of water on the rates of reduction. *Ultrason. Sonochem* 16, 387–391. doi:10.1016/J.ULTSONCH.2008.10.009

Olvera-Vargas, H., Wang, Z., Xu, J., and Lefebvre, O. (2022). Synergistic degradation of GenX (Hexafluoropropylene oxide dimer acid) by pairing graphene-coated Ni-foam and boron doped diamond electrodes. *Chem. Eng. J.* 430, 132686. doi:10.1016/j.cej.2021.132686

Panchangam, S. C., Lin, A. Y. C., Tsai, J. H., and Lin, C. F. (2009). Sonication-assisted photocatalytic decomposition of perfluorooctanoic acid. *Chemosphere* 75, 654–660. doi:10.1016/J.CHEMOSPHERE.2008.12.065

Panda, D., Sethu, V., and Manickam, S. (2019). Kinetics and mechanism of low-frequency ultrasound driven elimination of trace level aqueous perfluorooctanesulfonic acid and perfluorooctanoic acid. *Chem. Eng. Process. - Process Intensif.* 142, 107542. doi:10.1016/j.cep.2019.107542

Petrier, C., and Francony, A. (1997). Incidence of wave-frequency on the reaction rates during ultrasonic wastewater treatment. *Water Sci. Technol.* 35, 175–180. doi:10.1016/S0273-1223(97)00023-1

Pétrier, C., and Wei, Z. (2023). "The use of power ultrasound for water treatment," in *Power ultrasonics: applications of high-intensity ultrasound*. Second Edition, 797–815. doi:10.1016/B978-0-12-820254-8.00024-5

Pflieger, R., Nikitenko, S. I., Cairós, C., and Mettin, R. (2019). Characterization of cavitation bubbles and sonoluminescence. *SpringerBriefs Mol. Sci.* doi:10.1007/978-3-030-11717-7

Price, G. J., Ashokkumar, M., and Grieser, F. (2004). Sonoluminescence quenching of organic compounds in aqueous solution: frequency effects and implications for sonochemistry. *J. Am. Chem. Soc.* 126, 2755–2762. doi:10.1021/ja0389624

Ramos, P., Singh Kalra, S., Johnson, N. W., Khor, C. M., Borthakur, A., Cranmer, B., et al. (2022). Enhanced removal of per- and polyfluoroalkyl substances in complex matrices by polyDADMAC-coated regenerable granular activated carbon. *Environ. Pollut.* 294, 118603. doi:10.1016/j.envpol.2021.118603

Raso, J., Mañas, P., Pagán, R., and Sala, F. J. (1999). Influence of different factors on the output power transferred into medium by ultrasound. *Ultrason. Sonochem* 5, 157–162. doi:10.1016/S1350-4177(98)00042-X

Rodriguez-Freire, L., Balachandran, R., Sierra-Alvarez, R., and Keswani, M. (2015). Effect of sound frequency and initial concentration on the sonochemical degradation of perfluorooctane sulfonate (PFOS). *J. Hazard Mater* 300, 662–669. doi:10.1016/j.jhazmat.2015.07.077

Rodriguez-Freire, L., Abad-Fernández, N., Sierra-Alvarez, R., Hoppe-Jones, C., Peng, H., Giesy, J. P., et al. (2016). Sonochemical degradation of perfluorinated chemicals in aqueous film-forming foams. *J. Hazard Mater* 317, 275–283. doi:10.1016/j.jhazmat.2016.05.078

Rooze, J., Rebrov, E. V., Schouten, J. C., and Keurentjes, J. T. F. (2013). Dissolved gas and ultrasonic cavitation – a review. *Ultrason. Sonochem* 20, 1–11. doi:10.1016/J.ULTSONCH.2012.04.013

Saleh, L., Remot, M., Remaury, Q. B., Pardon, P., Labadi, P., Budzinski, H., et al. (2024). PFAS degradation by anodic electrooxidation: influence of BDD electrode configuration and presence of dissolved organic matter. *Chem. Eng. J.* 489, 151355. doi:10.1016/j.cej.2024.151355

Sekiguchi, K., Kudo, T., and Sankoda, K. (2017). Combined sonochemical and short-wavelength UV degradation of hydrophobic perfluorinated compounds. *Ultrason. Sonochem* 39, 87–92. doi:10.1016/j.ultsonch.2017.04.002

Shende, T., Andaluri, G., and Suri, R. P. S. (2019). Kinetic model for sonolytic degradation of non-volatile surfactants: perfluoroalkyl substances. *Ultrason. Sonochem* 51, 359–368. doi:10.1016/j.ultsonch.2018.08.028

Shende, T., Andaluri, G., and Suri, R. (2021a). Frequency-dependent sonochemical degradation of perfluoroalkyl substances and numerical analysis of cavity dynamics. *Sep. Purif. Technol.* 261, 118250. doi:10.1016/j.seppur.2020.118250

Shende, T., Andaluri, G., and Suri, R. (2021b). Power density modulated ultrasonic degradation of perfluoroalkyl substances with and without sparging argon. *Ultrason. Sonochem* 76, 105639. doi:10.1016/j.ultsonch.2021.105639

Shin-ichi Hatanaka, S. H., Kyuichi Yasui, K. Y., Toru Tuziuti, T. T., Teruyuki Kozuka, T. K., and Hideto Mitome, H. M. (2001). Quenching mechanism of multibubble sonoluminescence at excessive sound pressure. *Jpn. J. Appl. Phys.* 40, 3856. doi:10.1143/JJAP.40.3856

Sidnell, T., Wood, R. J., Hurst, J., Lee, J., and Bussemaker, M. J. (2022). Sonolysis of per- and poly fluoroalkyl substances (PFAS): a meta-analysis. *Ultrason. Sonochem* 87, 105944. doi:10.1016/j.ultsonch.2022.105944

Sidnell, T., Caceres Cobos, A. J., Hurst, J., Lee, J., and Bussemaker, M. J. (2023). Flow and temporal effects on the sonolytic defluorination of perfluorooctane sulfonic acid. *Ultrason. Sonochem* 101, 106667. doi:10.1016/j.ultsonch.2023.106667

Sidnell, T., Hurst, J., Lee, J., and Bussemaker, M. J. (2024). Increasing efficiency and treatment volumes for sonolysis of per- and poly-fluorinated substances, applied to aqueous film-forming foam. *Ultrason. Sonochem* 105, 106866. doi:10.1016/j.ultsonch.2024.106866

Singh Kalra, S., Cranmer, B., Dooley, G., Hanson, A. J., Maraviov, S., Mohanty, S. K., et al. (2021). Sonolytic destruction of Per- and polyfluoroalkyl substances in groundwater, aqueous film-forming foams, and investigation derived waste. *Chem. Eng. J.* 425, 131778. doi:10.1016/j.cej.2021.131778

Sivagami, K., Sharma, P., Karim, A. V., Mohanakrishna, G., Karthika, S., Divyapriya, G., et al. (2023). Electrochemical-based approaches for the treatment of forever chemicals: removal of perfluoroalkyl and polyfluoroalkyl substances (PFAS) from wastewater. *Sci. Total Environ.* 861, 160440. doi:10.1016/j.scitotenv.2022.160440

Sukhatskiy, Yu., Shepida, M., Sozanskyi, M., Znak, Z., and Gogate, P. R. (2023). Periodate-based advanced oxidation processes for wastewater treatment: a review. *Sep. Purif. Technol.* 304, 122305. doi:10.1016/j.seppur.2022.122305

Sunartio, D., Ashokkumar, M., and Grieser, F. (2005). The influence of Acoustic power on multibubble sonoluminescence in aqueous solution containing organic solutes. *J. Phys. Chem. B* 109, 20044–20050. doi:10.1021/JP052747N

Suslick, K. S. (1989). The chemical effects of ultrasound. *Sci. Am. Mag.* 260, 80–86. doi:10.1038/scientificamerican0289-80

Suslick, K. S., Didenko, Y., Fang, M. M., Hyeon, T., Kolbeck, K. J., McNamara, W. B., et al. (1999). Acoustic cavitation and its chemical consequences. *Philosophical Trans. R. Soc. Lond. Ser. A Math. Phys. Eng. Sci.* 357 (Issue 1751), 335–353. doi:10.1098/rsta.1999.0330

Tasca, A. L., Uwayezu, J. N., Carabante, I., and Kumpiene, J. (2025). Electrochemical remediation of PFAS by boron-doped diamond electrodes: a review. *J. Environ. Chem. Eng.* 13, 117044. doi:10.1016/J.JECE.2025.117044

Thompson, J., Eaglesham, G., Reungoat, J., Poussade, Y., Bartkow, M., Lawrence, M., et al. (2011). Removal of PFOS, PFOA and other perfluoroalkyl acids at water reclamation plants in south east Queensland Australia. *Chemosphere* 82, 9–17. doi:10.1016/j.chemosphere.2010.10.040

Uriakhil, M. A., Sidnell, T., De Castro Fernández, A., Lee, J., Ross, I., and Bussemaker, M. (2021). Per- and poly-fluoroalkyl substance remediation from soil and sorbents: a review of adsorption behaviour and ultrasonic treatment. *Chemosphere* 282, 131025. doi:10.1016/j.chemosphere.2021.131025

Vakili, M., Cagnetta, G., Deng, S., Wang, W., Gholami, Z., Gholami, F., et al. (2024). Regeneration of exhausted adsorbents after PFAS adsorption: a critical review. *J. Hazard Mater* 471, 134429. doi:10.1016/J.JHAZMAT.2024.134429

Vecitis, C. D., Park, H., Cheng, J., Mader, B. T., and Hoffmann, M. R. (2008a). Kinetics and mechanism of the sonolytic conversion of the aqueous perfluorinated surfactants, perfluorooctanoate (PFOA), and perfluorooctane sulfonate (PFOS) into inorganic products. *J. Phys. Chem. A* 112, 4261–4270. doi:10.1021/jp801081y

Vecitis, C. D., Park, H., Cheng, J., Mader, B. T., and Hoffmann, M. R. (2008b). Enhancement of perfluorooctanoate and perfluorooctanesulfonate activity at acoustic cavitation bubble interfaces. *J. Phys. Chem. C* 112, 16850–16857. doi:10.1021/jp804050p

Vecitis, C. D., Wang, Y. J., Cheng, J., Park, H., Mader, B. T., and Hoffmann, M. R. (2010). Sonochemical degradation of perfluorooctanesulfonate in aqueous film-forming foams. *Environ. Sci. Technol.* 44, 432–438. doi:10.1021/es902444r

Verma, S., Lee, T., Sahle-Demessie, E., Ateia, M., and Nadagouda, M. N. (2023). Recent advances on PFAS degradation *via* thermal and nonthermal methods. *Chem. Eng. J. Adv.* 13, 100411–100421. doi:10.1016/j.ceja.2022.100421

Wang, H., Cai, W.-W., Liu, W.-Z., Li, J.-Q., Wang, B., Yang, S.-C., et al. (2018). Application of sulfate radicals from ultrasonic activation: disintegration of extracellular polymeric substances for enhanced anaerobic fermentation of sulfate-containing waste-activated sludge. *Chem. Eng. J.* 352, 380–388. doi:10.1016/j.cej.2018.07.029

Wang, Y., Zhang, J., Zhang, W., Yao, J., Liu, J., He, H., et al. (2024). Electrostatic field in contact-electro-catalysis driven *c–f* bond cleavage of perfluoroalkyl substances. *Angew. Chem. Int. Ed.* 63, e202402440. doi:10.1002/anie.202402440

We, A. C. E., Zamyadi, A., Stickland, A. D., Clarke, B. O., and Freguia, S. (2024). A review of foam fractionation for the removal of per- and polyfluoroalkyl substances (PFAS) from aqueous matrices. *J. Hazard Mater* 465, 133182. doi:10.1016/j.jhazmat.2023.133182

Wood, R. J., Lee, J., and Bussemaker, M. J. (2017). A parametric review of sonochemistry: control and augmentation of sonochemical activity in aqueous solutions. *Ultrason. Sonochem* 38, 351–370. doi:10.1016/J.ULTSONCH.2017.03.030

Xiong, X., Shang, Y., Bai, L., Luo, S., Seviour, T. W., Guo, Z., et al. (2023). Complete defluorination of perfluorooctanoic acid (PFOA) by ultrasonic pyrolysis towards zero fluoro-pollution. *Water Res.* 235, 119829. doi:10.1016/j.watres.2023.119829

Yang, S., Sun, J., Hu, Y., Cheng, J., and Liang, X. (2013). Effect of vacuum ultraviolet on ultrasonic defluorination of aqueous perfluorooctanesulfonate. *Chem. Eng. J.* 234, 106–114. doi:10.1016/j.cej.2013.08.073

Yu, R. S., Yu, H. C., Yang, Y. F., and Singh, S. (2025). A global overview of Per- and polyfluoroalkyl substance regulatory strategies and their environmental impact. *Toxics* 13, 251. doi:10.3390/TOXICS13040251

Zark, M., and Dittmar, T. (2018). Universal molecular structures in natural dissolved organic matter. *Nat. Commun.* 9 (1 9), 3178. doi:10.1038/s41467-018-05665-9

Zhao, H., Zhang, G., and Zhang, Q. (2014). MnO2/CeO2 for catalytic ultrasonic degradation of methyl Orange. *Ultrason. Sonochem* 21, 991–996. doi:10.1016/J.ULTSONCH.2013.12.002

Zhou, M., Yusof, N. S. M., and Ashokkumar, M. (2013). Correlation between sonochemistry and sonoluminescence at various frequencies. *RSC Adv.* 3, 9319–9324. doi:10.1039/C3RA41123K